PROCEEDINGS OF SCIENCE

Performance and extensions of the central data acquisition system for Phase II of the Pierre Auger Observatory

Paul Filip[ab,*] **for the Pierre Auger Collaboration**[c]

[a] *Institute for Astroparticle Physics, Karlsruhe Institute for Technology*
Hermann-von-Helmholtz Platz 1, 76344 Eggenstein-Leopoldshafen, Germany

[b] *Instituto de Tecnologias en Deteccion y Astroparticulas, Universidad Nacional de General San Martín*
Av. Gral. Paz 1499, B1650 Buenos Aires, Argentina

[c] *Observatorio Pierre Auger, Av. San Martín Norte 304, 5613 Malargüe, Argentina*
Full Author List https://www.auger.org/archive/authors_icrc_2025.html

E-mail: spokespersons@auger.org

The Pierre Auger Observatory is a hybrid detector designed to observe and study ultra-high-energy particles of extraterrestrial origin. With its 27 fluorescence telescopes and over 1600 autonomously operating water-Cherenkov detectors spread over an area of 3000 km^2, it is world-leading in terms of exposure to cosmic rays and offers an unparalleled window into the physical processes that happen at energy scales unattainable by particle accelerators on Earth.
Measurement information of candidate air-shower events from all associated detectors and telescopes is collected at a central data-acquisition system located in the nearby town of Malargüe, and processed for higher-level physics analysis. On top of this, data for monitoring the long-term stability and operation of the observatory is forwarded to the central server as well.
In this work, we briefly review the central data-acquisition system of the Pierre Auger Observatory. We examine the rates, efficiencies, and purity of detected events for Phase II of the Pierre Auger Observatory and compare them to performance parameters during Phase I. We detail challenges in the event detection up until now and present recent changes in the central data acquisition system and local station software that aim to streamline the data acquisition chain.

39th International Cosmic Ray Conference (ICRC2025)
15–24 July 2025
Geneva, Switzerland

ICRC 2025
The Astroparticle Physics Conference
Geneva July 15-24, 2025

*Speaker

PoS(ICRC2025)254

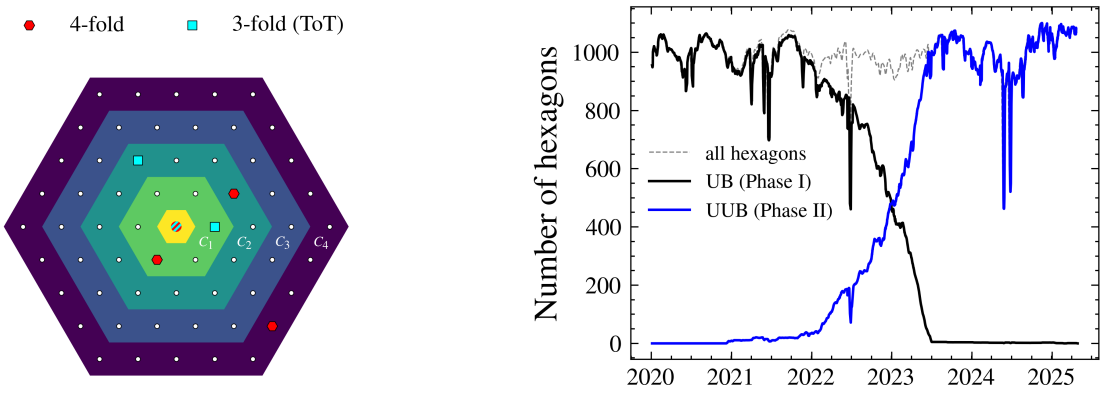

(a) **(b)**

Figure 1: a The event trigger is based on the n nearest neighbors, organized in hexagonal rings around a central triggered station. For the 3-fold trigger 2ToTC_1&3C_2 (cyan), at least one nearest neighbor (in C_1), as well as one next to nearest neighbor (in C_2), must be present. On top of this, only T2 triggers of a specific type are considered during pattern matching. The $2C_1$&$3C_2$&$4C_4$ (red) considers all station-level triggers but requires at least one additional station that can be as far as a 4th nearest neighbor. b Weekly average number of hexagons during the AugerPrime upgrade, split into upgraded stations (blue), and stations with original electronics (black). Bad weather during the winter months is responsible for large-scale array shutdowns.

1. Introduction

The Pierre Auger Observatory covers an area of roughly 3000 km^2 and is the world's largest detector for extensive air showers stemming from cosmic rays of ultra-high energies. The observatory consists of 27 UV-sensitive telescopes, called the Fluorescence Detector (FD), and > 1600 stations that comprise the Surface Detector (SD). The immense size of the observatory, coupled with its remote location in the Argentinian pampa, poses unique challenges. For example, a single SD station collects data with a sampling rate of 120 MHz, which results in a theoretical bandwidth of the order of TB/s for the SD alone. Of course, it is not feasible to transfer this amount of data over the distances present in the SD array. Instead, data from a station must pass through a hierarchical trigger system before being sent to a Central Data Acquisition System (CDAS). In this way, the data transfer rate[1] between the CDAS ↔ station can be limited to < 150 B/s. An exact discussion of the communication system and the software implementation is given in Ref. [1].

The lowest level in the trigger hierarchy is the station level. Every SD station independently monitors its detector data for several trigger conditions. If a trigger condition is met, the station sends a station-level trigger (T2) with a microsecond timestamp to the CDAS. The CDAS scans all incoming T2s for spatio-temporal coincidences, which are usually caused by air showers induced by cosmic rays. Two patterns are considered when searching for coincidences: the 3-fold 2ToTC_1&3C_2 pattern and the more permissive 4-fold $2C_1$&$3C_2$&$4C_4$ pattern (ref. Figure 1a and [2]). If such a pattern is recognized, the CDAS issues an event-level trigger (T3) and requests data from the participating triggered stations to collect all information related to an event.

[1] Including also diagnostic information about the detector performance.

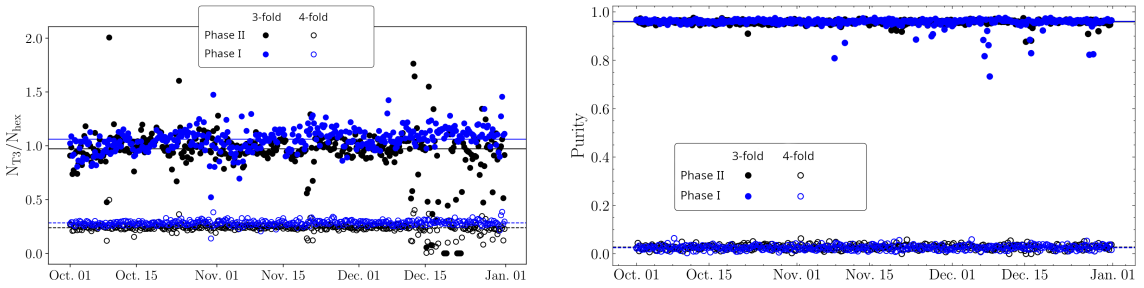

(a) **(b)**

Figure 2: a Number of T3s per hexagon, separated by trigger mode for Phase I data (blue) and for Phase II data (black). The Phase I data was collected from October 2021 to December 2021. The Phase II data stems from the same timespan in 2024 and displays high variance at the end of the DAQ period, likely due to thunderstorms. b The T3 purity of the aforementioned dataset. Horizontal lines give the mean T3 purity.

With the AugerPrime upgrade, the Pierre Auger Observatory achieves a higher discrimination on the primary particle mass and enters Phase II of its data collection. During the upgrade, all of the SD station electronics have been upgraded from a Unified Board (UB, 10-bit ADC sampled at 40 MHz) to the Upgraded Unified Board (UUB, 11-bit ADC sampled at 120 MHz).

With the higher resolution of the UUB data, the event detection chain changes in principle from the ground up. However, steps have been taken to ensure the backward compatibility of Phase I and Phase II triggers [3]. We show this in Section 2 by compiling a preliminary CDAS performance report for Phase II and comparing it with the performance during Phase I. We highlight challenges present in the event detection chain and discuss how they can be solved from Section 3 onward.

2. CDAS Performance Phase I + Phase II

A number of parameters have proven useful to monitor the low-level performance of the CDAS. For example, the T3 frequency should resemble the rate with which air showers impinge on the SD array. Since the latter is constant for UHECRs, the former should be (with invariant trigger settings) too constant. Of course, this is assuming a detector of constant area, which was not the case for the SD during Phase II commissioning (cf. Figure 1b).

Table 1: CDAS performance parameters. Event rates are given in no. of T3s per hexagon per day.

	Phase I	II (prelim.)	Δ / %
3-fold rate	4.24	3.89	-8
3-fold purity	0.961	0.960	±0
4-fold rate	1.13	0.95	-16
4-fold purity	0.025	0.028	+9
SD uptime	0.96 [2]	0.957	±0

The number of SD unit cells, called hexagons, consisting of one central station and its six nearest neighbors increases (decreases) for the UUB (UB) array as individual stations are upgraded. As the UUB array grows, it detects more air shower events. We therefore define *T3 rate* as the frequency of (types of) T3s, normalized to the number of hexagons that operate simultaneously in the SD array.

After registering a T3 and requesting event data from stations, the CDAS also applies physics-based quality checks, storing their outcome alongside the event information. These checks filter out random coincidences of T2s and deliver T3 events that are almost entirely formed by extensive air showers. Thus, a measure of the background contamination in the T3 dataset is given by the fraction of events that pass the higher-level selection criteria. This is the *T3 purity*. Lastly, we quantify the duty cycle of the SD array during an observation period by splitting it into intervals of 15 min. We build the *SD uptime* by dividing the number of intervals that do not have T3 events by the number of all intervals.

To compare the CDAS performance between Phase I and Phase II, we collect all T3 events from October to December in the years 2021 and 2024. We choose the specific periods due to the good weather[2] and the overall stable operation of the SD. Moreover, the UB array in 2021 and the UUB array in 2024 have a comparable size and thus exposure (cf. Figure 1b).

This serves as a tentative analysis to gauge the CDAS performance in Phase II. Quality cuts have not been applied to the data. The systematics of the analysis have not been estimated but are assumed to be of the order of 10 %. In any case, the results presented in this section are meant to be understood as preliminary. The calculated T3 rate and purity for Phase I and Phase II are displayed in Figure 2a and Figure 2b. Their mean values and the SD uptime over the entire DAQ period are also listed in Table 1.

We observe a slight decrease in T3 rates for both the 3-fold and the 4-fold trigger modes. The difference in the performance of Phase I and Phase II is probably due to the compatibility mode in which the SD stations operate in Phase II. In compatibility mode, the UUB emulates the UB electronics readout process and applies the same station-level trigger algorithms to the filtered and downsampled data that were in use in Phase I. Evidently, the emulation is not perfect, as the T3 rates are not backwards compatible and overall, fewer events are observed.

The T3 purity remains unchanged for the 3-fold trigger and increases slightly for the 4-fold trigger. The SD uptime is very similar for both DAQ periods and implies that no significant downtimes were observed during the detector upgrade, both for the UB and UUB array.

3. Sources of transient noise

Several sources of noise are and have been present in the T2/T3 datasets for Phase II. Although the underlying effects and problems have, in part, been known since Phase I already, their impact is amplified with the advent of the higher data resolution that the new station electronics offer.

3.1 Local Sidereal Time

Figure 3a shows the number of working UUB hexagons in the array for the year 2023. A very careful inspection of the data reveals a pattern that persists throughout the year. Each day, shortly after sunrise, the number of functioning hexagons drops by up to 40%, causing a decrease in exposure of 0.1% over the entire year on average. This is caused by individual stations reporting a very high T2 rate, which results in the CDAS issuing a reset command in the station and temporarily removing it from the active DAQ (Ref. [4]).

[2]Thunderstorms and heavy rain were reported over the observatory at the end of 2024.

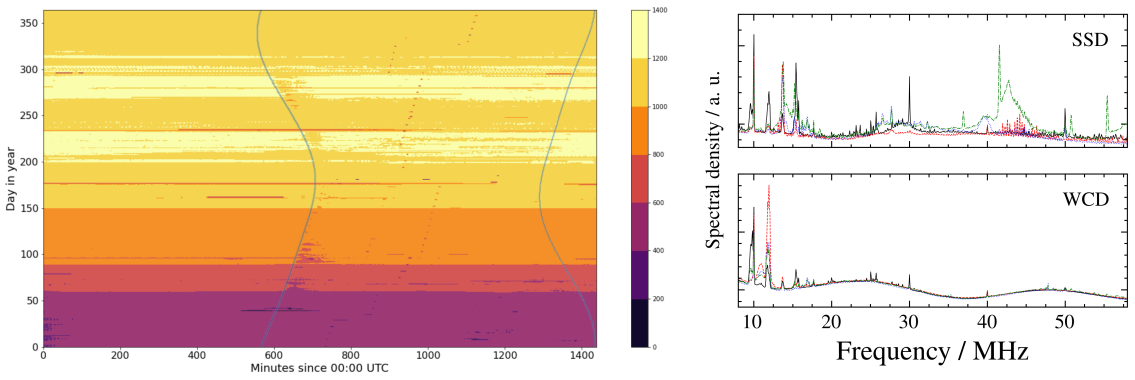

(a) **(b)**

Figure 3: a Number of fully functional hexagons in the UUB array for 2023. The sinusoidal blue lines mark the time of sunrise and sunset. b The spectral density of the SSD (top) and WCD (bottom) detector for background data of various UUB stations. Several sharp peaks demonstrate the systematic influence of electronic noise. The data was recorded in 2022-11 (black, red) and 2023-03 (green, blue).

As such, the noise present in the stations is only indirectly observed via a degraded performance of the SD. The effect is clearly related to the local sidereal time in the UUB array. The Tank Power Control Board (TPCB) has been theorized to be responsible for the burst in the trigger rate when charging station batteries during the morning hours. The problem can be mitigated in the laboratory by equipping the TPCB with diodes and capacitors. With all TPCBs in the field being upgraded in this fashion and the implementation of the trace-cleaning algorithm in Section 4, the behavior is no longer observed.

3.2 Electronic Noise

To gauge the presence of electronic noise in the detectors, we analyze background data of the SD. The data set on hand originates from two different measurements in November 2022 and March 2023 and contains 394.4 s of randomly sampled detector data collected from four stations. It is divided into sets of 2048 consecutive samples that measure 17 µs in duration. During the DAQ, 5000 such traces are acquired in quick succession and written to disk. The writing introduces a considerable delay, resulting in roughly 60 s of data being stored in a 22 h interval.

We calculate the FFT of the data on a trace level, applying a Hanning window to minimize spectral leakage. Figure 3b shows the mean FFT, grouped by SSD and WCD, for all four stations.

Several frequency bands are clearly polluted by artificial signal constituents. In unfortunate circumstances, electronic noise can trigger a T2 trigger, as shown in Figure 5. The erroneously sent T2 can then form a T3 pattern with coincident T2s at neighboring stations. This results in the false detection of an air shower event and decreases the T3 purity of the CDAS.

3.3 Thunderstorms

The largest source of detector instabilities is lightning activity. Both in Phase I and Phase II, a spike in the T3 rate and a subsequent drop in the T3 purity are observed during and in the wake of thunderstorms, as shown in Figure 4. During these periods, the SD stations exhibit an elevated rate of T2 triggers. More importantly, T2 triggers from neighboring stations are highly correlated

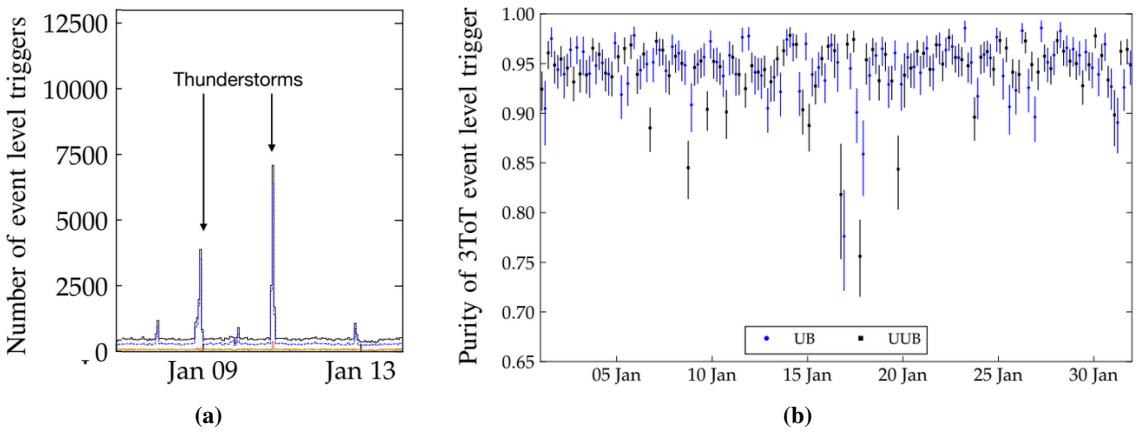

Figure 4: a A large number of 3-fold T3s is recorded during periods with thunderstorms, as indicated by the arrows. b The corresponding 3-fold T3 purity rate measures a drop coincident with the weather period.

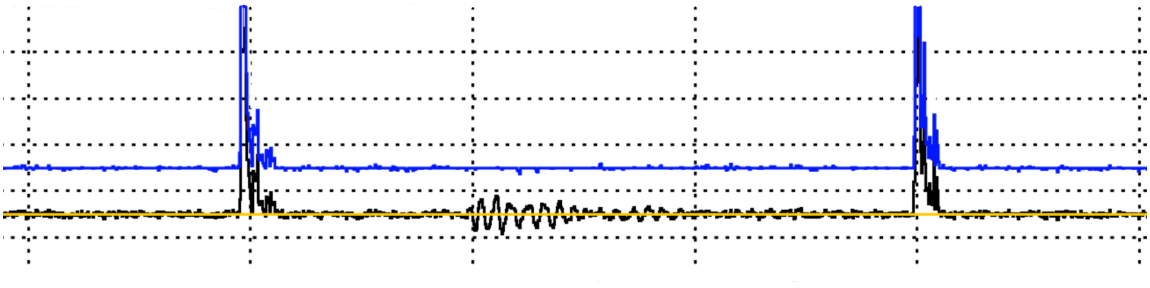

Figure 5: An erroneously triggered WCD trace (black) displays electronic noise in the form of a 10 MHz oscillation around the baseline (orange) between two sub-threshold muon pulses. The blue trace is the output of a trace-cleaning algorithm using the black trace as input. The effect of the electronic noise is mitigated

in time, as they are likely caused by the same electric discharge. Consequently, the CDAS identifies many more T3 events than during nominal operation. Since the communication between the CDAS and SD stations is bandwidth-limited, only one to two T3 requests can be issued to the SD array every second. This represents a bottleneck that results in the buildup of a large T3 queue during thunderstorms. The CDAS naively iterates through the T3 queue and requests data from a station often hours after the event happened.[3] Such stale events block the acquisition of new, real air shower events and drop the T3 purity and SD uptime considerably. The estimated effect on the duty cycle of the UB array is $\sim 2\,\%$. The UUB, with its higher resolution, is more susceptible to lightning-induced triggering. The drop in the SD duty cycle for Phase II reads 5%. The algorithm presented in Section 5 partially fixes this issue.

4. Improved trigger algorithm

A new trigger algorithm has been in operation in the UUB electronics since August 2024, which aims to diminish the sensitivity of the T2 algorithms to electronic noise. This is achieved by

[3]The SD stations save T2 data for $\sim 30\,$s.

first filtering symmetric oscillations in the trace and then providing the established triggers with the conditioned version of the detector information.

To detect oscillations, the trace conditioner employs a sliding window algorithm that continuously scans the last 15 samples (125 ns) of the trace data. For each sample b_i, the algorithm determines the minimum $\wedge$ and the maximum $\vee$ for the three right- and leftmost bins $b_{i\pm7}$, $b_{i\pm6}$, $b_{i\pm5}$. It checks for a sinusoidal pattern in the samples b_i, $\{\wedge, \vee\}_{\text{left}}^{\text{right}}$ around the baseline B (Ref. [5]), that is to say, the conditioner tests whether Eqs. (1) or (2) are satisfied.

$$\wedge_{\text{right}} + 4\,\text{ADC} < B < b_i, \qquad \wedge_{\text{left}} + 4\,\text{ADC} < B < b_i. \qquad \text{Case :} \qquad (1)$$

$$\vee_{\text{right}} - 4\,\text{ADC} > B > b_i, \qquad \vee_{\text{left}} - 4\,\text{ADC} > B > b_i. \qquad \text{Case :} \qquad (2)$$

In the Eqs. (1-2), a dead band of $2\sigma_B = 4\,\text{ADC}$ counts is used. Oscillations below this threshold are not considered spurious and are not altered. If a sinusoidal pattern is found, the conditioned trace is calculated according to Eqs. (3-4). If no pattern is found, it is $b_i^{\text{cond.}} = b_i$.

$$b_i^{\text{cond.}} = b_i + \left(\max(\wedge_{\text{left}}, \wedge_{\text{right}}) - B\right) + 0.5\,\text{ADC} \qquad \text{Case :} \qquad (3)$$

$$b_i^{\text{cond.}} = b_i + \left(\min(\vee_{\text{left}}, \vee_{\text{right}}) - B\right) - 0.5\,\text{ADC} \qquad \text{Case :} \qquad (4)$$

5. Rejection of stale T3s

An algorithmically simple method for mitigating the effect of stale T3s on the T3 rate and purity has been in operation at the CDAS since January 2025. Before sending a T3 request to stations, a maximum age check is applied at the CDAS level. If the T2 triggers forming the T3 coincidence are older than the cutoff time, the CDAS will reject the request and discard it instead of sending it to the SD array. The schematic operation and its advantages over the naive iteration of the T3 queue are shown in Figure 6. The projected improvement in the duty cycle of the SD array is up to 5%.

6. Conclusion

The Central Data Acquisition System (CDAS) is the main computing facility of the Pierre Auger Observatory. Most importantly, it is responsible for recognizing extensive air shower events from spatio-temporal coincidences of T2 triggers and communicating with candidate stations. The CDAS performed this task reliably during Phase I of data collection, as shown by several performance parameters that are monitored throughout the operation. These performance parameters remain largely unchanged after the AugerPrime detector upgrade.

With the higher resolution of detector data, several sources of noise have impacted the event detection quality in non-trivial ways. The effects leading to losses in T3 rates and purities have been studied in depth and solutions have been deployed that mitigate their impact on data quality. The CDAS, in its current state, represents a well-tested system that is prepared for the challenges that come with the AugerPrime detector upgrade and is expected to improve its Phase I performance.

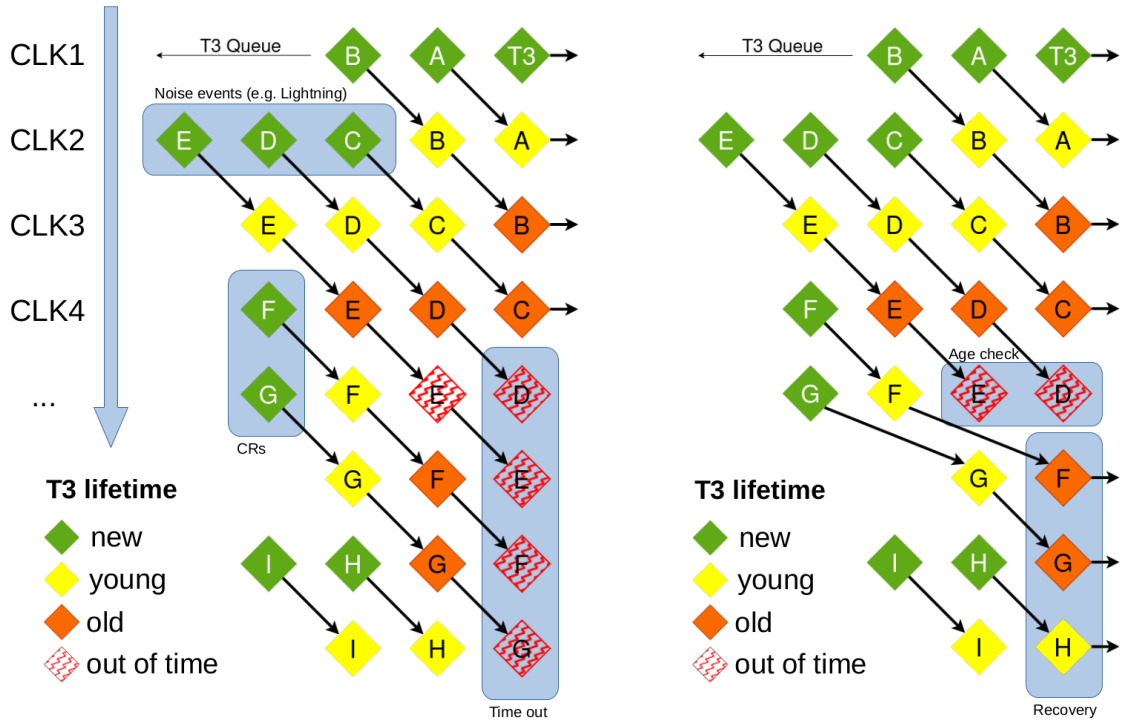

Figure 6: a A large backlog of T3s (caused, e.g., by lightning) can cripple the CDAS performance for much longer than the actual bad weather period. b A simple age check rejects T3 requests that are out of time. The CDAS recovers much faster as a consequence.

References

[1] R. Sato [Pierre Auger Collaboration], PoS **ICRC2023** (2023) 373.
[2] J. Abraham *et al.*, Nucl. Instrum. Methods A, **613** (2010) 029-039.
[3] A. Castellina [Pierre Auger Collaboration], EPJ Web Conf. **210** (2019) 06002.
[4] C. Bonifazi [Pierre Auger Collaboration], JINST **ICRC2013** (2013) 019-022.
[5] X. Bertou *et al.*, Nucl. Instrum. Methods A, **568** (2006) 839-846.

PoS(ICRC2025)254

The Pierre Auger Collaboration

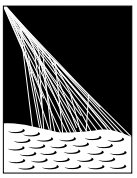

A. Abdul Halim[13], P. Abreu[70], M. Aglietta[53,51], I. Allekotte[1], K. Almeida Cheminant[78,77], A. Almela[7,12], R. Aloisio[44,45], J. Alvarez-Muñiz[76], A. Ambrosone[44], J. Ammerman Yebra[76], G.A. Anastasi[57,46], L. Anchordoqui[83], B. Andrada[7], L. Andrade Dourado[44,45], S. Andringa[70], L. Apollonio[58,48], C. Aramo[49], E. Arnone[62,51], J.C. Arteaga Velázquez[66], P. Assis[70], G. Avila[11], E. Avocone[56,45], A. Bakalova[31], F. Barbato[44,45], A. Bartz Mocellin[82], J.A. Bellido[13], C. Berat[35], M.E. Bertaina[62,51], M. Bianciotto[62,51], P.L. Biermann[a], V. Binet[5], K. Bismark[38,7], T. Bister[77,78], J. Biteau[36,i], J. Blazek[31], J. Blümer[40], M. Boháčová[31], D. Boncioli[56,45], C. Bonifazi[8], L. Bonneau Arbeletche[22], N. Borodai[68], J. Brack[f], P.G. Brichetto Orchera[7,40], F.L. Briechle[41], A. Bueno[75], S. Buitink[15], M. Buscemi[46,57], M. Büsken[38,7], A. Bwembya[77,78], K.S. Caballero-Mora[65], S. Cabana-Freire[76], L. Caccianiga[58,48], F. Campuzano[6], J. Caraça-Valente[82], R. Caruso[57,46], A. Castellina[53,51], F. Catalani[19], G. Cataldi[47], L. Cazon[76], M. Cerda[10], B. Čermáková[40], A. Cermenati[44,45], J.A. Chinellato[22], J. Chudoba[31], L. Chytka[32], R.W. Clay[13], A.C. Cobos Cerutti[6], R. Colalillo[59,49], R. Conceição[70], G. Consolati[48,54], M. Conte[55,47], F. Convenga[44,45], D. Correia dos Santos[27], P.J. Costa[70], C.E. Covault[81], M. Cristinziani[43], C.S. Cruz Sanchez[3], S. Dasso[4,2], K. Daumiller[40], B.R. Dawson[13], R.M. de Almeida[27], E.-T. de Boone[43], B. de Errico[27], J. de Jesús[7], S.J. de Jong[77,78], J.R.T. de Mello Neto[27], I. De Mitri[44,45], J. de Oliveira[18], D. de Oliveira Franco[42], F. de Palma[55,47], V. de Souza[20], E. De Vito[55,47], A. Del Popolo[57,46], O. Deligny[33], N. Denner[31], L. Deval[53,51], A. di Matteo[51], C. Dobrigkeit[22], J.C. D'Olivo[67], L.M. Domingues Mendes[16,70], Q. Dorosti[43], J.C. dos Anjos[16], R.C. dos Anjos[26], J. Ebr[31], F. Ellwanger[40], R. Engel[38,40], I. Epicoco[55,47], M. Erdmann[41], A. Etchegoyen[7,12], C. Evoli[44,45], H. Falcke[77,79,78], G. Farrar[85], A.C. Fauth[22], T. Fehler[43], F. Feldbusch[39], A. Fernandes[70], M. Fernandez[14], B. Fick[84], J.M. Figueira[7], P. Filip[38,7], A. Filipčič[74,73], T. Fitoussi[40], B. Flaggs[87], T. Fodran[77], A. Franco[47], M. Freitas[70], T. Fujii[86,h], A. Fuster[7,12], C. Galea[77], B. García[6], C. Gaudu[37], P.L. Ghia[33], U. Giaccari[47], F. Gobbi[10], F. Gollan[7], G. Golup[1], M. Gómez Berisso[1], P.F. Gómez Vitale[11], J.P. Gongora[11], J.M. González[1], N. González[7], D. Góra[68], A. Gorgi[53,51], M. Gottowik[40], F. Guarino[59,49], G.P. Guedes[23], L. Gülzow[40], S. Hahn[38], P. Hamal[31], M.R. Hampel[7], P. Hansen[3], V.M. Harvey[13], A. Haungs[40], T. Hebbeker[41], C. Hojvat[d], J.R. Hörandel[77,78], P. Horvath[32], M. Hrabovský[32], T. Huege[40,15], A. Insolia[57,46], P.G. Isar[72], M. Ismaiel[77,78], P. Janecek[31], V. Jilek[31], K.-H. Kampert[37], B. Keilhauer[40], A. Khakurdikar[77], V.V. Kizakke Covilakam[7,40], H.O. Klages[40], M. Kleifges[39], J. Köhler[40], F. Krieger[41], M. Kubatova[31], N. Kunka[39], B.L. Lago[17], N. Langner[41], N. Leal[7], M.A. Leigui de Oliveira[25], Y. Lema-Capeans[76], A. Letessier-Selvon[34], I. Lhenry-Yvon[33], L. Lopes[70], J.P. Lundquist[73], M. Mallamaci[60,46], D. Mandat[31], P. Mantsch[d], F.M. Mariani[58,48], A.G. Mariazzi[3], I.C. Mariş[14], G. Marsella[60,46], D. Martello[55,47], S. Martinelli[40,7], M.A. Martins[76], H.-J. Mathes[40], J. Matthews[g], G. Matthiae[61,50], E. Mayotte[82], S. Mayotte[82], P.O. Mazur[d], G. Medina-Tanco[67], J. Meinert[37], D. Melo[7], A. Menshikov[39], C. Merx[40], S. Michal[31], M.I. Micheletti[5], L. Miramonti[58,48], M. Mogarkar[68], S. Mollerach[1], F. Montanet[35], L. Morejon[37], K. Mulrey[77,78], R. Mussa[51], W.M. Namasaka[37], S. Negi[31], L. Nellen[67], K. Nguyen[84], G. Nicora[9], M. Niechciol[43], D. Nitz[84], D. Nosek[30], A. Novikov[87], V. Novotny[30], L. Nožka[32], A. Nucita[55,47], L.A. Núñez[29], J. Ochoa[7,40], C. Oliveira[20], L. Östman[31], M. Palatka[31], J. Pallotta[9], S. Panja[31], G. Parente[76], T. Paulsen[37], J. Pawlowsky[37], M. Pech[31], J. Pękala[68], R. Pelayo[64], V. Pelgrims[14], L.A.S. Pereira[24], E.E. Pereira Martins[38,7], C. Pérez Bertolli[7,40], L. Perrone[55,47], S. Petrera[44,45], C. Petrucci[56], T. Pierog[40], M. Pimenta[70], M. Platino[7], B. Pont[77], M. Pourmohammad Shahvar[60,46], P. Privitera[86], C. Priyadarshi[68], M. Prouza[31], K. Pytel[69], S. Querchfeld[37], J. Rautenberg[37], D. Ravignani[7], J.V. Reginatto Akim[22], A. Reuzki[41], J. Ridky[31], F. Riehn[76,j], M. Risse[43], V. Rizi[56,45], E. Rodriguez[7,40], G. Rodriguez Fernandez[50], J. Rodriguez Rojo[11], S. Rossoni[42], M. Roth[40], E. Roulet[1], A.C. Rovero[4], A. Saftoiu[71], M. Saharan[77], F. Salamida[56,45], H. Salazar[63], G. Salina[50], P. Sampathkumar[40], N. San Martin[82], J.D. Sanabria Gomez[29], F. Sánchez[7], E.M. Santos[21], E. Santos[31], F. Sarazin[82], R. Sarmento[70], R. Sato[11], P. Savina[44,45], V. Scherini[55,47], H. Schieler[40], M. Schimassek[33], M. Schimp[37], D. Schmidt[40], O. Scholten[15,b], H. Schoorlemmer[77,78], P. Schovánek[31], F.G. Schröder[87,40], J. Schulte[41], T. Schulz[31], S.J. Sciutto[3], M. Scornavacche[7], A. Sedoski[7], A. Segreto[52,46], S. Sehgal[37], S.U. Shivashankara[73], G. Sigl[42], K. Simkova[15,14], F. Simon[39], R. Šmída[86], P. Sommers[e], R. Squartini[10], M. Stadelmaier[40,48,58], S. Stanič[73], J. Stasielak[68], P. Stassi[35], S. Strähnz[38], M. Straub[41], T. Suomijärvi[36], A.D. Supanitsky[7], Z. Svozilikova[31], K. Syrokvas[30], Z. Szadkowski[69], F. Tairli[13], M. Tambone[59,49], A. Tapia[28], C. Taricco[62,51], C. Timmermans[78,77], O. Tkachenko[31], P. Tobiska[31], C.J. Todero Peixoto[19], B. Tomé[70], A. Travaini[10], P. Travnicek[31], M. Tueros[3], M. Unger[40], R. Uzeiroska[37], L. Vaclavek[32], M. Vacula[32], I. Vaiman[44,45], J.F. Valdés Galicia[67], L. Valore[59,49], P. van Dillen[77,78], E. Varela[63], V. Vašíčková[37], A. Vásquez-Ramírez[29], D. Veberič[40], I.D. Vergara Quispe[3], S. Verpoest[87], V. Verzi[50], J. Vicha[31], J. Vink[80], S. Vorobiov[73], J.B. Vuta[31], C. Watanabe[27], A.A. Watson[c], A. Weindl[40], M. Weitz[37], L. Wiencke[82], H. Wilczyński[68], B. Wundheiler[7], B. Yue[37], A. Yushkov[31], E. Zas[76], D. Zavrtanik[73,74], M. Zavrtanik[74,73]

[1] Centro Atómico Bariloche and Instituto Balseiro (CNEA-UNCuyo-CONICET), San Carlos de Bariloche, Argentina
[2] Departamento de Física and Departamento de Ciencias de la Atmósfera y los Océanos, FCEyN, Universidad de Buenos Aires and CONICET, Buenos Aires, Argentina
[3] IFLP, Universidad Nacional de La Plata and CONICET, La Plata, Argentina
[4] Instituto de Astronomía y Física del Espacio (IAFE, CONICET-UBA), Buenos Aires, Argentina
[5] Instituto de Física de Rosario (IFIR) – CONICET/U.N.R. and Facultad de Ciencias Bioquímicas y Farmacéuticas U.N.R., Rosario, Argentina
[6] Instituto de Tecnologías en Detección y Astropartículas (CNEA, CONICET, UNSAM), and Universidad Tecnológica Nacional – Facultad Regional Mendoza (CONICET/CNEA), Mendoza, Argentina
[7] Instituto de Tecnologías en Detección y Astropartículas (CNEA, CONICET, UNSAM), Buenos Aires, Argentina
[8] International Center of Advanced Studies and Instituto de Ciencias Físicas, ECyT-UNSAM and CONICET, Campus Miguelete – San Martín, Buenos Aires, Argentina
[9] Laboratorio Atmósfera – Departamento de Investigaciones en Láseres y sus Aplicaciones – UNIDEF (CITEDEF-CONICET), Argentina
[10] Observatorio Pierre Auger, Malargüe, Argentina
[11] Observatorio Pierre Auger and Comisión Nacional de Energía Atómica, Malargüe, Argentina
[12] Universidad Tecnológica Nacional – Facultad Regional Buenos Aires, Buenos Aires, Argentina
[13] University of Adelaide, Adelaide, S.A., Australia
[14] Université Libre de Bruxelles (ULB), Brussels, Belgium
[15] Vrije Universiteit Brussels, Brussels, Belgium
[16] Centro Brasileiro de Pesquisas Fisicas, Rio de Janeiro, RJ, Brazil
[17] Centro Federal de Educação Tecnológica Celso Suckow da Fonseca, Petropolis, Brazil
[18] Instituto Federal de Educação, Ciência e Tecnologia do Rio de Janeiro (IFRJ), Brazil
[19] Universidade de São Paulo, Escola de Engenharia de Lorena, Lorena, SP, Brazil
[20] Universidade de São Paulo, Instituto de Física de São Carlos, São Carlos, SP, Brazil
[21] Universidade de São Paulo, Instituto de Física, São Paulo, SP, Brazil
[22] Universidade Estadual de Campinas (UNICAMP), IFGW, Campinas, SP, Brazil
[23] Universidade Estadual de Feira de Santana, Feira de Santana, Brazil
[24] Universidade Federal de Campina Grande, Centro de Ciencias e Tecnologia, Campina Grande, Brazil
[25] Universidade Federal do ABC, Santo André, SP, Brazil
[26] Universidade Federal do Paraná, Setor Palotina, Palotina, Brazil
[27] Universidade Federal do Rio de Janeiro, Instituto de Física, Rio de Janeiro, RJ, Brazil
[28] Universidad de Medellín, Medellín, Colombia
[29] Universidad Industrial de Santander, Bucaramanga, Colombia
[30] Charles University, Faculty of Mathematics and Physics, Institute of Particle and Nuclear Physics, Prague, Czech Republic
[31] Institute of Physics of the Czech Academy of Sciences, Prague, Czech Republic
[32] Palacky University, Olomouc, Czech Republic
[33] CNRS/IN2P3, IJCLab, Université Paris-Saclay, Orsay, France
[34] Laboratoire de Physique Nucléaire et de Hautes Energies (LPNHE), Sorbonne Université, Université de Paris, CNRS-IN2P3, Paris, France
[35] Univ. Grenoble Alpes, CNRS, Grenoble Institute of Engineering Univ. Grenoble Alpes, LPSC-IN2P3, 38000 Grenoble, France
[36] Université Paris-Saclay, CNRS/IN2P3, IJCLab, Orsay, France
[37] Bergische Universität Wuppertal, Department of Physics, Wuppertal, Germany
[38] Karlsruhe Institute of Technology (KIT), Institute for Experimental Particle Physics, Karlsruhe, Germany
[39] Karlsruhe Institute of Technology (KIT), Institut für Prozessdatenverarbeitung und Elektronik, Karlsruhe, Germany
[40] Karlsruhe Institute of Technology (KIT), Institute for Astroparticle Physics, Karlsruhe, Germany
[41] RWTH Aachen University, III. Physikalisches Institut A, Aachen, Germany
[42] Universität Hamburg, II. Institut für Theoretische Physik, Hamburg, Germany
[43] Universität Siegen, Department Physik – Experimentelle Teilchenphysik, Siegen, Germany
[44] Gran Sasso Science Institute, L'Aquila, Italy
[45] INFN Laboratori Nazionali del Gran Sasso, Assergi (L'Aquila), Italy
[46] INFN, Sezione di Catania, Catania, Italy
[47] INFN, Sezione di Lecce, Lecce, Italy
[48] INFN, Sezione di Milano, Milano, Italy
[49] INFN, Sezione di Napoli, Napoli, Italy
[50] INFN, Sezione di Roma "Tor Vergata", Roma, Italy
[51] INFN, Sezione di Torino, Torino, Italy

[52] Istituto di Astrofisica Spaziale e Fisica Cosmica di Palermo (INAF), Palermo, Italy
[53] Osservatorio Astrofisico di Torino (INAF), Torino, Italy
[54] Politecnico di Milano, Dipartimento di Scienze e Tecnologie Aerospaziali , Milano, Italy
[55] Università del Salento, Dipartimento di Matematica e Fisica "E. De Giorgi", Lecce, Italy
[56] Università dell'Aquila, Dipartimento di Scienze Fisiche e Chimiche, L'Aquila, Italy
[57] Università di Catania, Dipartimento di Fisica e Astronomia "Ettore Majorana", Catania, Italy
[58] Università di Milano, Dipartimento di Fisica, Milano, Italy
[59] Università di Napoli "Federico II", Dipartimento di Fisica "Ettore Pancini", Napoli, Italy
[60] Università di Palermo, Dipartimento di Fisica e Chimica "E. Segrè", Palermo, Italy
[61] Università di Roma "Tor Vergata", Dipartimento di Fisica, Roma, Italy
[62] Università Torino, Dipartimento di Fisica, Torino, Italy
[63] Benemérita Universidad Autónoma de Puebla, Puebla, México
[64] Unidad Profesional Interdisciplinaria en Ingeniería y Tecnologías Avanzadas del Instituto Politécnico Nacional (UPIITA-IPN), México, D.F., México
[65] Universidad Autónoma de Chiapas, Tuxtla Gutiérrez, Chiapas, México
[66] Universidad Michoacana de San Nicolás de Hidalgo, Morelia, Michoacán, México
[67] Universidad Nacional Autónoma de México, México, D.F., México
[68] Institute of Nuclear Physics PAN, Krakow, Poland
[69] University of Łódź, Faculty of High-Energy Astrophysics,Łódź, Poland
[70] Laboratório de Instrumentação e Física Experimental de Partículas – LIP and Instituto Superior Técnico – IST, Universidade de Lisboa – UL, Lisboa, Portugal
[71] "Horia Hulubei" National Institute for Physics and Nuclear Engineering, Bucharest-Magurele, Romania
[72] Institute of Space Science, Bucharest-Magurele, Romania
[73] Center for Astrophysics and Cosmology (CAC), University of Nova Gorica, Nova Gorica, Slovenia
[74] Experimental Particle Physics Department, J. Stefan Institute, Ljubljana, Slovenia
[75] Universidad de Granada and C.A.F.P.E., Granada, Spain
[76] Instituto Galego de Física de Altas Enerxías (IGFAE), Universidade de Santiago de Compostela, Santiago de Compostela, Spain
[77] IMAPP, Radboud University Nijmegen, Nijmegen, The Netherlands
[78] Nationaal Instituut voor Kernfysica en Hoge Energie Fysica (NIKHEF), Science Park, Amsterdam, The Netherlands
[79] Stichting Astronomisch Onderzoek in Nederland (ASTRON), Dwingeloo, The Netherlands
[80] Universiteit van Amsterdam, Faculty of Science, Amsterdam, The Netherlands
[81] Case Western Reserve University, Cleveland, OH, USA
[82] Colorado School of Mines, Golden, CO, USA
[83] Department of Physics and Astronomy, Lehman College, City University of New York, Bronx, NY, USA
[84] Michigan Technological University, Houghton, MI, USA
[85] New York University, New York, NY, USA
[86] University of Chicago, Enrico Fermi Institute, Chicago, IL, USA
[87] University of Delaware, Department of Physics and Astronomy, Bartol Research Institute, Newark, DE, USA

---

[a] Max-Planck-Institut für Radioastronomie, Bonn, Germany
[b] also at Kapteyn Institute, University of Groningen, Groningen, The Netherlands
[c] School of Physics and Astronomy, University of Leeds, Leeds, United Kingdom
[d] Fermi National Accelerator Laboratory, Fermilab, Batavia, IL, USA
[e] Pennsylvania State University, University Park, PA, USA
[f] Colorado State University, Fort Collins, CO, USA
[g] Louisiana State University, Baton Rouge, LA, USA
[h] now at Graduate School of Science, Osaka Metropolitan University, Osaka, Japan
[i] Institut universitaire de France (IUF), France
[j] now at Technische Universität Dortmund and Ruhr-Universität Bochum, Dortmund and Bochum, Germany

Acknowledgments

The successful installation, commissioning, and operation of the Pierre Auger Observatory would not have been possible without the strong commitment and effort from the technical and administrative staff in Malargüe. We are very grateful to the following agencies and organizations for financial support:

Argentina – Comisión Nacional de Energía Atómica; Agencia Nacional de Promoción Científica y Tecnológica (ANPCyT); Consejo Nacional de Investigaciones Científicas y Técnicas (CONICET); Gobierno de la Provincia de Mendoza; Municipalidad de Malargüe; NDM Holdings and Valle Las Leñas; in gratitude for their continuing cooperation over land access; Australia – the Australian Research Council; Belgium – Fonds de la Recherche Scientifique (FNRS); Research Foundation Flanders (FWO), Marie Curie Action of the European Union Grant No. 101107047; Brazil – Conselho Nacional de Desenvolvimento Científico e Tecnológico (CNPq); Financiadora de Estudos e Projetos (FINEP); Fundação de Amparo à Pesquisa do Estado de Rio de Janeiro (FAPERJ); São Paulo Research Foundation (FAPESP) Grants No. 2019/10151-2, No. 2010/07359-6 and No. 1999/05404-3; Ministério da Ciência, Tecnologia, Inovações e Comunicações (MCTIC); Czech Republic – GACR 24-13049S, CAS LQ100102401, MEYS LM2023032, CZ.02.1.01/0.0/0.0/16_013/0001402, CZ.02.1.01/0.0/0.0/18_046/0016010 and CZ.02.1.01/0.0/0.0/17_049/0008422 and CZ.02.01.01/00/22_008/0004632; France – Centre de Calcul IN2P3/CNRS; Centre National de la Recherche Scientifique (CNRS); Conseil Régional Ile-de-France; Département Physique Nucléaire et Corpusculaire (PNC-IN2P3/CNRS); Département Sciences de l'Univers (SDU-INSU/CNRS); Institut Lagrange de Paris (ILP) Grant No. LABEX ANR-10-LABX-63 within the Investissements d'Avenir Programme Grant No. ANR-11-IDEX-0004-02; Germany – Bundesministerium für Bildung und Forschung (BMBF); Deutsche Forschungsgemeinschaft (DFG); Finanzministerium Baden-Württemberg; Helmholtz Alliance for Astroparticle Physics (HAP); Helmholtz-Gemeinschaft Deutscher Forschungszentren (HGF); Ministerium für Kultur und Wissenschaft des Landes Nordrhein-Westfalen; Ministerium für Wissenschaft, Forschung und Kunst des Landes Baden-Württemberg; Italy – Istituto Nazionale di Fisica Nucleare (INFN); Istituto Nazionale di Astrofisica (INAF); Ministero dell'Università e della Ricerca (MUR); CETEMPS Center of Excellence; Ministero degli Affari Esteri (MAE), ICSC Centro Nazionale di Ricerca in High Performance Computing, Big Data and Quantum Computing, funded by European Union NextGenerationEU, reference code CN_00000013; México – Consejo Nacional de Ciencia y Tecnología (CONACYT) No. 167733; Universidad Nacional Autónoma de México (UNAM); PAPIIT DGAPA-UNAM; The Netherlands – Ministry of Education, Culture and Science; Netherlands Organisation for Scientific Research (NWO); Dutch national e-infrastructure with the support of SURF Cooperative; Poland – Ministry of Education and Science, grants No. DIR/WK/2018/11 and 2022/WK/12; National Science Centre, grants No. 2016/22/M/ST9/00198, 2016/23/B/ST9/01635, 2020/39/B/ST9/01398, and 2022/45/B/ST9/02163; Portugal – Portuguese national funds and FEDER funds within Programa Operacional Factores de Competitividade through Fundação para a Ciência e a Tecnologia (COMPETE); Romania – Ministry of Research, Innovation and Digitization, CNCS-UEFISCDI, contract no. 30N/2023 under Romanian National Core Program LAPLAS VII, grant no. PN 23 21 01 02 and project number PN-III-P1-1.1-TE-2021-0924/TE57/2022, within PNCDI III; Slovenia – Slovenian Research Agency, grants P1-0031, P1-0385, I0-0033, N1-0111; Spain – Ministerio de Ciencia e Innovación/Agencia Estatal de Investigación (PID2019-105544GB-I00, PID2022-140510NB-I00 and RYC2019-027017-I), Xunta de Galicia (CIGUS Network of Research Centers, Consolidación 2021 GRC GI-2033, ED431C-2021/22 and ED431F-2022/15), Junta de Andalucía (SOMM17/6104/UGR and P18-FR-4314), and the European Union (Marie Sklodowska-Curie 101065027 and ERDF); USA – Department of Energy, Contracts No. DE-AC02-07CH11359, No. DE-FR02-04ER41300, No. DE-FG02-99ER41107 and No. DE-SC0011689; National Science Foundation, Grant No. 0450696, and NSF-2013199; The Grainger Foundation; Marie Curie-IRSES/EPLANET; European Particle Physics Latin American Network; and UNESCO.